

**NASA TECHNICAL NOTE**



**NASA TN D-3553**

**NASA TN D-3553**

*c. 1*

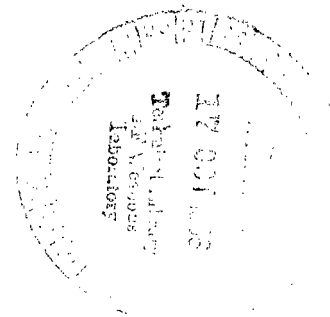


LOAN COPY: RET  
AFWL (WLII  
KIRTLAND AFB, N. MEX.

# STABILITY OF INTERMIXING OF HIGH-VELOCITY VAPOR WITH ITS SUBCOOLED LIQUID IN COCURRENT STREAMS

*by William H. Westendorf and William F. Brown*

*Lewis Research Center  
Cleveland, Ohio*



NATIONAL AERONAUTICS AND SPACE ADMINISTRATION • WASHINGTON, D. C. • OCTOBER 1966



STABILITY OF INTERMIXING OF HIGH-VELOCITY VAPOR WITH  
ITS SUBCOOLED LIQUID IN COCURRENT STREAMS

By William H. Westendorf and William F. Brown

Lewis Research Center  
Cleveland, Ohio

NATIONAL AERONAUTICS AND SPACE ADMINISTRATION

---

For sale by the Clearinghouse for Federal Scientific and Technical Information  
Springfield, Virginia 22151 – Price \$1.00

# STABILITY OF INTERMIXING OF HIGH-VELOCITY VAPOR WITH ITS SUBCOOLED LIQUID IN COCURRENT STREAMS

by William H. Westendorf and William F. Brown

Lewis Research Center

## SUMMARY

The instabilities that occur with the intermixing of a vapor with its subcooled liquid were studied with steam and water flowing horizontally through a 1-inch-diameter tube near atmospheric pressure. Oscillographic traces of pressures, temperatures, and flow rates together with high-speed movies and photographs recorded the disturbances. Three modes of instability were found: (1) random high-frequency fluctuations; (2) regular low-frequency oscillations; and (3) interface excursions. The amplitude of the fluctuations was directly proportional to the coolant inlet subcooling and flow rate. Data plots of the coolant inlet temperature as a function of the mass flow rate ratio define the regions of regular oscillatory instability and interface excursions. The amplitude of the oscillations was inversely proportional to the flow rate ratio. The similarities between these instabilities and those of subcooled boiling are examined.

## INTRODUCTION

Stability problems are encountered often in two-phase (vapor-liquid) flow devices. The presence of the second phase may arise through either partial changing of phase, as in boiling or condensing, or direct intermixing of two phases, such as in a contact condenser. The intermixing may also be unintentional; for example, when one radiator becomes inoperable in a space power system that contains multiple, parallel convective condensers, intermixing will occur at the condensate return manifold. In the contact condenser (sometimes called a jet or spray condenser), the vapor and subcooled liquid are injected together. Within a relatively short distance, the mixing and resultant condensation have taken place. This process of condensing vapor directly on the subcooled liquid is not new; it has been used in steam powerplants, in locomotives, and more re-

cently in torpedoes. However, very few data on the stability of such devices are available. In the studies of references 1 and 2, instabilities of pressure, interface, and flow were observed in jet condensers. The instabilities were not systematically investigated, however. Instabilities have also been experimentally observed in boilers and other types of condensers. These were characterized by either irregular high-frequency pressure fluctuations or regular low-frequency oscillations of pressure, interface, and flow (refs. 3 to 8). In recent years, these stability problems have resulted in more research on two-phase flow stability in general.

The purpose of this investigation was to observe, record, and distinguish any instabilities encountered in the intermixing of a high-velocity vapor with its subcooled liquid in a closed system. The effects of certain variables on the amplitudes and the inception points of the instabilities were also studied. The variables included the coolant inlet subcooling and coolant flow rate and the pressure drop in the coolant line. In this way, some insight into condenser stability and its relation to other two-phase stability problems, such as subcooled boiling, could be gained.

Research was conducted at the Lewis Research Center in a closed-loop stainless-steel system with a test section of 1-inch-outside-diameter by 12-inch-long transparent glass. Oscillographic traces of pressures, temperatures, and flow rates, synchronized with high-speed movies and photographs, were used to record the oscillations. Data plots of the coolant inlet temperature  $T_0$  as a function of the mass flow rate ratio (symbols defined in appendix A) show the regions of stability, and other plots show the inverse proportionality of the amplitude of the pressure oscillations and the mass flow rate ratio. The effect of a pressure drop in the coolant inlet line was investigated, along with similarities between the instabilities of this contact condenser and those of subcooled boiling. Appendix B describes the type of oscillations that occurred in the multitube, forced flow boiler and the method used to alleviate these disturbances.

## APPARATUS

### Flow System

The facility used was a closed-loop system constructed of stainless steel (including pumps). Figure 1 is a schematic diagram of the system, including the locations of pertinent instrumentation and the approximate plumbing dimensions. All heat exchangers were commercially built stainless-steel shell-and-tube single-pass designs. The electric preheater was an immersion type.

The test coolant was circulated by a nearly constant flow gear pump powered by a variable-speed drive that gave a flow range of 0.1 to 10 gallons per minute at 100-pound-



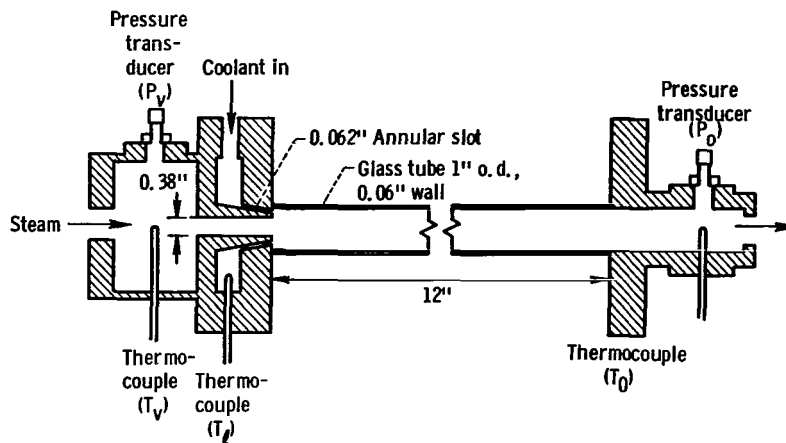


Figure 2 - Basic test section.

per-square-inch head rise. The boiler feed pump was also a gear pump, which produced nearly constant flow at head rises up to 100 pounds per square inch. The pump was powered by a variable-speed drive that gave a flow range of 0 to 1.0 gallon per minute.

A small cooler was provided upstream of this boiler-feed pump to prevent harmful cavitation. The variable-speed drives provided fine continuous control over the full flow range. Because of the close tolerances of these gear pumps, a filter was installed upstream of the pumps to remove any solid particles. The boiler was heated by hot water that was circulated through the boiler heating loop by a constant-speed high-temperature centrifugal pump with a capacity of 2 to 20 gallons per minute at a constant head rise of 20 pounds per square inch. The hot water was pressurized to 115 pounds per square inch absolute and heated by the 100-pound-per-square-inch-absolute building supply steam.

## Test Section

The test section consisted of a 1-inch-outside-diameter 12-inch-long glass tube. As shown in figure 2, a brass coolant and vapor injector nozzle assembly was installed at the inlet of the tube; it could, however, be removed for alterations. Pressures and temperatures were measured at the stainless-steel inlet and exit sections. The glass portion was sealed by compressed square O-rings around the tube, which still allowed for axial expansion. A transparent shield was provided for protection of the personnel.

## Instrumentation

The fluid bulk temperatures at various stations in the loop were measured by copper-

constantan thermocouples and recorded on multipoint self-balancing potentiometers that were calibrated periodically with a standard potentiometer. The overall accuracy of the temperature measurements was estimated to be  $\pm 0.5^{\circ}\text{F}$ .

The average fluid pressures were monitored at several locations in the loops with Bourdon tube gages. The instantaneous pressures at the test section, steam inlet and outlet, and the boiler steam outlet were first measured with flush-mounted strain-gage-type transducers, which had a range of  $\pm 25$  pounds per square inch differential (one side was open to the atmosphere) and an accuracy of 1 percent of full scale for frequencies up to 2000 cps. Later in the program, on the test section, variable reluctance transducers were used, which had a range of 0 to 50 pounds per square inch absolute with an accuracy of 0.5 percent of full scale for frequencies up to 600 cps. These transducers were connected to the test section by 1-inch-long 0.125-inch-diameter tubes. A 12-inch 0- to 100-pound-per-square-inch Bourdon tube gage was used to calibrate the transducers.

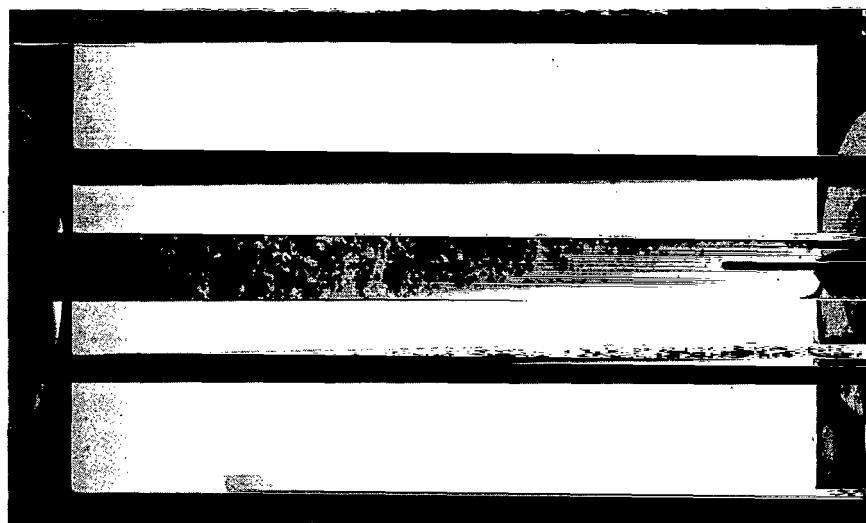
The various flow rates were measured by turbine-type flowmeters that had an accuracy of 0.5 percent and a response time of 3 milliseconds. The flowmeter pulses were read on a digital frequency counter, but they could also be converted to millivolt signals for oscillographic recording. An eight-channel pen recorder with variable chart speeds and direct-current amplifiers recorded the signals from thermocouples, pressure transducers, and flowmeters. The frequency response was flat to 60 cps at 50 chart lines peak-to-peak and flat to 120 cps at 10 chart lines peak-to-peak. Two marginal timing pens were provided, one of which was used to synchronize the motion pictures with the data.

Photographic equipment was used to facilitate the analytical work. Motion pictures were taken by both high-speed cameras, capable of 16 000 pictures per second, and normal-speed cameras, at 16 to 40 frames per second. A camera - stroboscopic-light combination was used for still shots.

## PROCEDURE

The system was initially flushed with demineralized water and evacuated. While under vacuum, the loops were filled with demineralized, partially deaerated water (10 to 12 ppm by weight). Further degassing was accomplished in the system itself by heating the liquid to near its saturation temperature and venting the freed noncondensable gases to the atmosphere.

Deaerating was continued until the gas analyzation indicated an air content of 5 ppm (by weight) or below. Nevertheless, even at 5 ppm, there was an extremely high number of small air bubbles immediately downstream of the condensing interface. This high number is to be expected in a region near saturation because of the high density difference



(a) Before deaerating; air content, 14 ppm by weight.



(b) After deaerating; air content, 4.5 ppm by weight.

Figure 3. - Test section before and after deaerating.

between air and water. Photographs of the fluid taken before and after deaerating are shown in figure 3; both photographs were taken at similar conditions of flow rates, pressure, and temperature.

Prior to the taking of data, the system was brought up to the desired conditions and held for 10 to 15 minutes to assure a steady state. Temperatures, pressures, and flow rates were recorded at this steady-state condition. The coolant temperature was then allowed to rise slowly and eventually reached the temperature at which low frequency, pressure, and interface oscillations occurred. The coolant temperature rise was accomplished by a slow decrease in the cold, city-water flow rate to the cooler that was downstream of the test section. During this time interval, the pertinent temperatures,



pressures, and flow rates were recorded continuously on the oscillograph. The transient run was complete when the coolant temperature was high enough so that the interface completely departed from the test section. At the conclusion of each run, the coolant temperature was returned to the required value for the next run. Although this was the normal operating procedure, it was possible to initiate the oscillations by attempting to maintain a constant coolant temperature and slowly decreasing the coolant flow rate. The points of instability were the same as for the normal procedure. The alternate method of decreasing the flow rate was not used extensively, because a change in the coolant flow rate would affect the coolant temperature. This interdependency of the flow rate and the temperature was due to the particular closed-loop design of the facility.

The ranges of test variables for the investigation were as follows:

Steam flow rate, lb/hr . . . . .	44 to 148
Coolant flow rate, lb/hr . . . . .	480 to 2800
Steam temperature, °F . . . . .	up to 250
Coolant subcooling, °F . . . . .	up to 160
Coolant inlet velocity, ft/sec . . . . .	2 to 18
Vapor inlet velocity, ft/sec . . . . .	330 to 840
Vapor inlet pressure, psia . . . . .	16 to 27

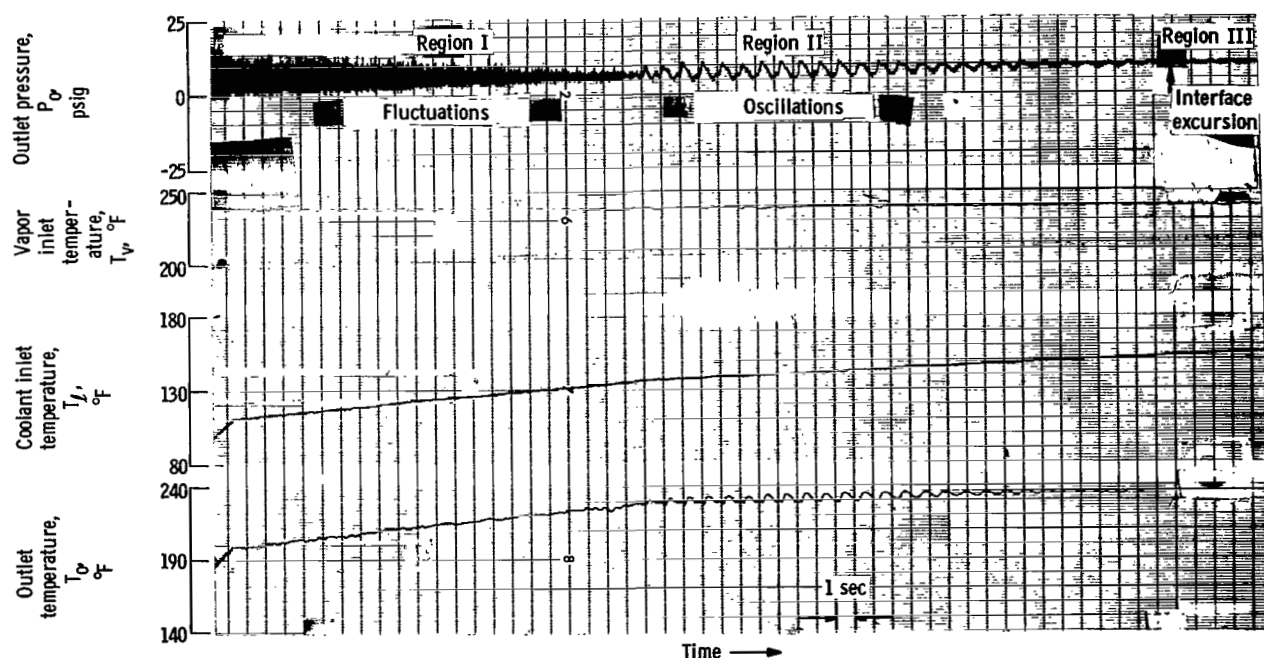


Figure 4. - Typical oscillograph traces for three regions of instability.

## RESULTS AND DISCUSSION

The instabilities associated with the intermixing of the vapor and the subcooled liquid in a flowing stream were recorded as oscillographic traces of pressures, temperatures, and flow rates. The oscillographic traces of temperatures and pressure for a typical run are shown in figure 4. The outlet pressure trace  $P_o$  goes through three stages or modes of instability, indicated by regions I, II, and III, as the coolant inlet temperature is slowly increased. The other variables are held constant, as previously mentioned. Region I of the pressure trace is characterized by high-frequency (50 to 200 cps) irregular fluctuations; as the coolant temperature continues to rise, the amplitude of the high frequencies subsides and region II on the oscillographic pressure trace begins. The second region on the trace appears as low-frequency pressure oscillations, which had associated interface and coolant inlet flow oscillations. As the coolant temperature continues to rise, the low-frequency (1 to 10 cps) oscillations increase in amplitude to some maximum and then decay to zero, at which time region III begins. Region III is distinguished by a steady (nonoscillatory) pressure trace indicative of a complete loss or downstream excursion of both the interface and the associated steady annular flow pattern; that is, complete condensation is no longer possible in a relatively short distance. The interface excursion is referred to as the third type of instability, the excursive mode.

### Region I - High-Frequency Pressure Fluctuations

As long as the outlet temperature was well below saturation, the outlet pressure trace was quite irregular or noisy. The signal was of irregular amplitude and frequency (50 to 200 cps); however, as can be seen in figures 4 and 5, there is enough regularity that some measurement of the peak-to-peak values can be averaged by eye. The amplitude of the fluctuations decreases as the coolant inlet temperature  $T_l$  increases, as can be seen in the oscillograph trace in figure 4. The effect of the coolant inlet temperature is shown in figure 6, where the amplitude of the fluctuations is plotted against the coolant inlet subcooling for four flow rates. The amplitude of the fluctuations decreases not only with decreasing inlet subcooling but also with decreasing coolant flow rate. Thus, with

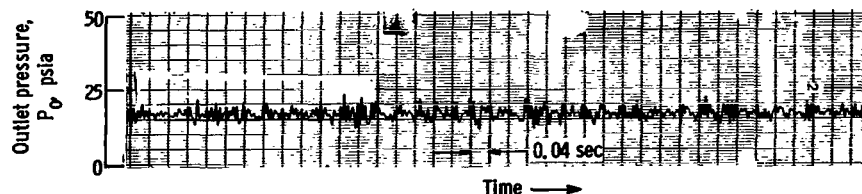


Figure 5. - High-frequency pressure fluctuations recorded at high oscillograph chart speed.

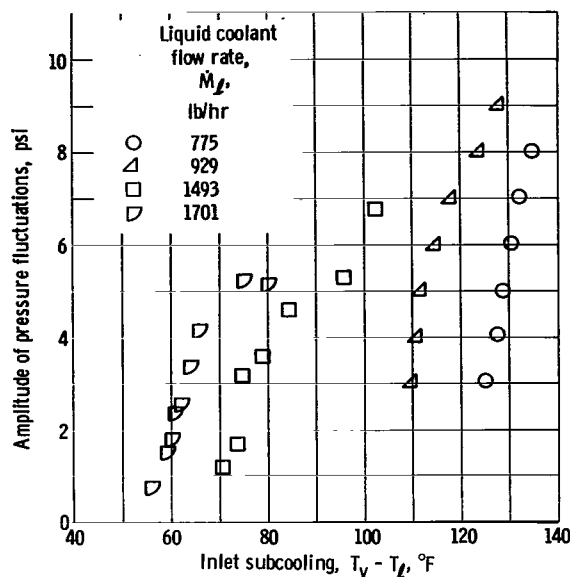


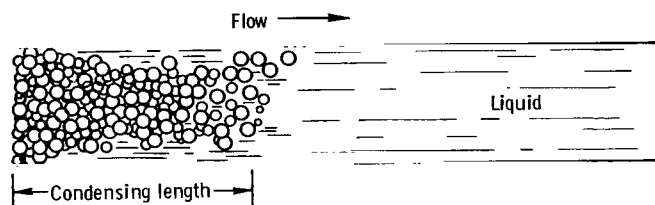
Figure 6. - Amplitude of pressure fluctuations (region I) as function of inlet coolant subcooling at various coolant flow rates. Constant vapor flow rate,  $73.5 \pm 0.5$  pound per hour; saturation pressure, approximately 23.5 pounds per square inch absolute.

other variables held constant, neither the subcooling nor the flow rate alone determines the amplitude of the fluctuations, but rather the combination of the two.

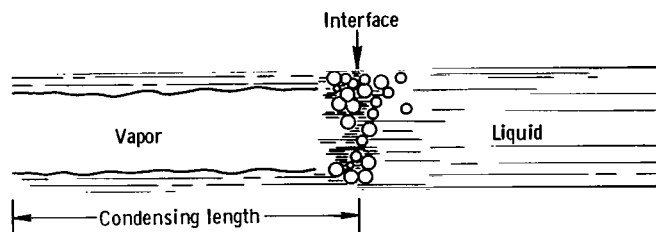
It is believed that these fluctuations are a result of vapor void collapse because of the attenuation with increasing  $T_l$  and the ultimate disappearance of the disturbances as the saturation temperature is approached. Similar phenomena have been reported in subcooled nucleate boiling studies such as reference 3.

## Region II - Low-Frequency Pressure and Interface Oscillations

When the high-frequency pulses begin to disappear, the low-frequency (1 to 10 cps) pressure and interface oscillations begin to appear. Visual observations and the motion pictures taken during this onset period indicate that the cloudy or bubbly condensing region near the injection nozzle slowly grows to a length of 2 to 3 inches; at this point there is always a sudden transition from the bubbly or mixed flow to a definite annular flow with a clearly defined interface (fig. 7). Once the annular pattern has formed, the condensing length grows much more rapidly; that is, the interface moves rapidly downstream. The interface then begins to decelerate, stops, and returns sud-



(a) Prior to oscillations; bubbly or mixed condensing region.



(b) After onset of oscillations; annular condensing region.

Figure 7. - Flow patterns immediately before and after onset of oscillations.

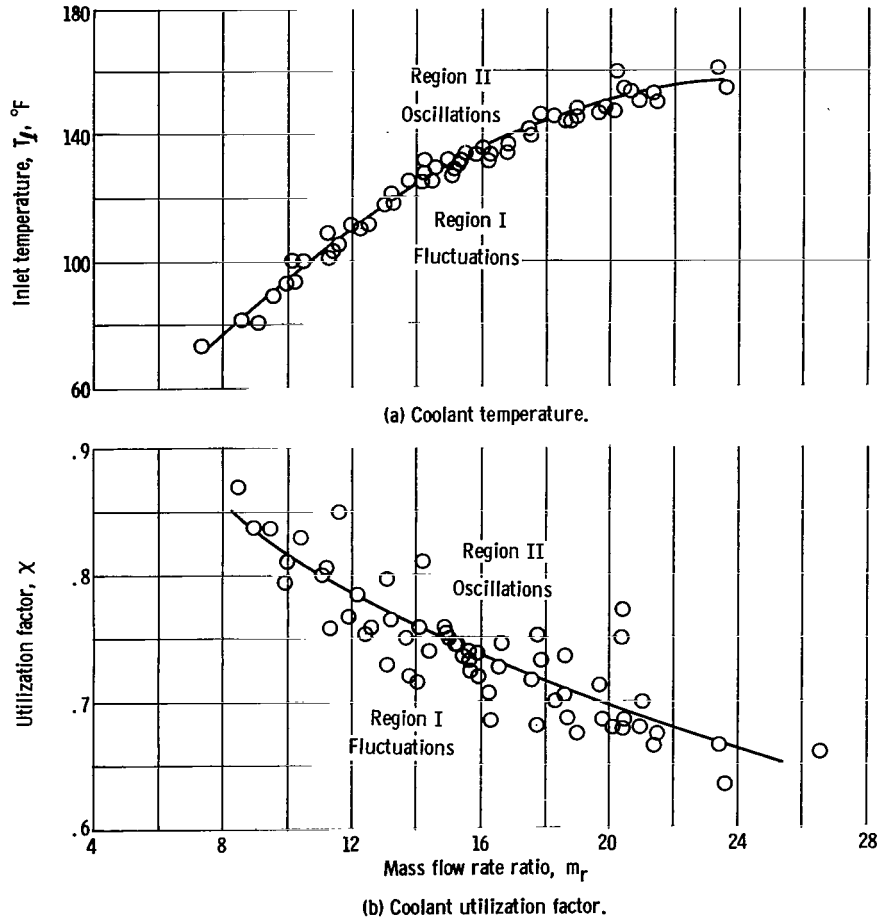


Figure 8. - Stability plots at onset of low-frequency oscillations. Saturation pressure, approximately 17 pounds per square inch absolute.

denly to the entrance region of the condenser, where the cycle repeats itself. Thus, the oscillations are characterized by the condensing length or annular region alternately growing to some maximum and then diminishing or collapsing. The oscillatory stability boundary is shown in figure 8(a), where the nonoscillatory region is below the curve. In this figure, the coolant inlet temperature  $T_l$  at which the onset of oscillations occurs is plotted against the ratio of coolant to vapor mass flow rate  $m_r$ . This inception temperature increases with increasing flow rate ratios. The data for the inception of oscillations are replotted in the form of the coolant utilization factor  $\chi$  as a function of the flow rate ratio  $m_r$  in figure 8(b). The coolant utilization factor  $\chi$  is the ratio of the actual enthalpy change of the coolant to the maximum possible change, or  $\chi = (T_o - T_l) / (T_v - T_l)$ . In a space power system, higher values of  $\chi$  indicate lower radiator weights, since  $T_o$  approaches  $T_v$  as  $\chi$  goes to unity, and  $T_o$  is the radiator inlet temperature. High values of  $\chi$  also indicate little excess coolant flow and, hence, little excess coolant pumping power. Figure 8(b) shows that the value of  $\chi$  at the onset of oscillatory instability decreases as the flow rate ratio increases.

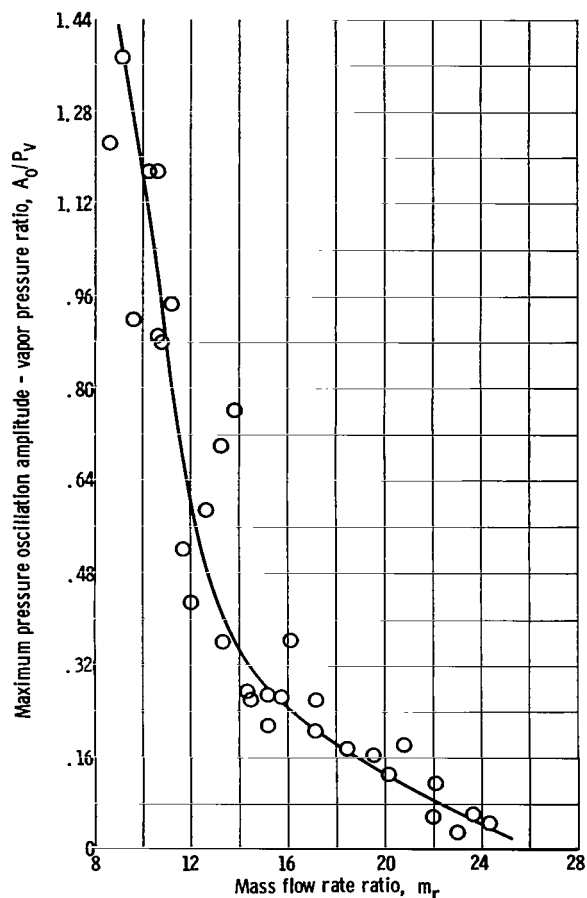


Figure 9. - Ratio of maximum amplitude of pressure oscillations to inlet vapor pressure as function of mass flow rate ratio. Saturation pressure, approximately 25 pounds per square inch absolute.

As  $T_l$  continues to increase during a run (see fig. 4, p. 7), the low-frequency amplitude grows to some maximum, which was as high as 34 pounds per square inch peak-to-peak at a mean pressure level near atmospheric pressure. This maximum amplitude of the outlet  $A_0$  is inversely proportional to  $m_r$ , as shown in figure 9. The curve indicates that, at some higher  $m_r$ , the low-frequency oscillations would fail to appear as  $T_l$  increases. This was verified experimentally. Therefore, for a given vapor flow rate, some relatively high coolant flow rate was found such that, as  $T_l$  was increased, the only noticeable phenomena were the subsiding of the high-frequency fluctuations and the eventual excursion of the interface.

It is obvious then that lower flow rate ratios are undesirable in two respects: (1) the stable region is reduced, that is, the oscillations occur at lower coolant inlet temperatures, and (2) the amplitudes of the oscillations are larger.

A series of runs was conducted early in the study to determine how a pressure drop

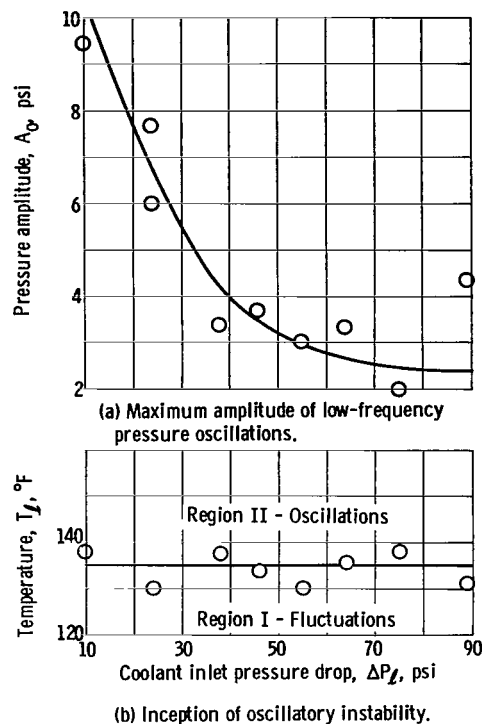


Figure 10. - Effect of coolant inlet pressure drop on amplitude of low-frequency oscillations and on inception of oscillatory instability. Saturation pressure, approximately 17 pounds per square inch absolute; mass flow rate ratio,  $15 \pm 4$  percent.

in the coolant line  $\Delta P_\ell$  would affect the stability. Increasing the pressure drop did reduce the peak-to-peak amplitude of the low-frequency outlet pressure oscillations, although this attenuating effect appeared to be diminishing, if not negligible, at pressure drops greater than 35 pounds per square inch, as shown in figure 10. The coolant pump, however, was capable of only 100 pounds per square inch of output pressure, and at this maximum permissible pressure drop, the pressure and interface oscillations still occurred. With the low pressure drops (10 and 24 psi) (fig. 10(a)), the coolant flow was oscillated with the test section pressure with variations of approximately 8 and 4 percent of the mean, respectively. At pressure drops above 25 pounds per square inch, no discernable flow oscillations were recorded. Consequently, for the succeeding runs, the pressure drop in the coolant inlet line was held at a constant and relatively high value (35, 70, or 90 psi) for each series of runs to ensure steady coolant flow rates. Furthermore, the  $\Delta P_\ell$  had no significant effect on the value of  $T_\ell$  at the onset of oscillations, as shown in figure 10(b).

### Region III - Interface Excursions

Previously it was stated that, at some value of coolant inlet temperature  $T_\ell$ , complete condensing could no longer be effected in a relatively short distance; the interface would move downstream out of the test section and would not return until the coolant temperature was lowered. Photographs of such excursions are shown in figure 11. As discussed in the section on region II, at some high flow rate ratio the excursions were not preceded by the regular low-frequency oscillations. For the oscillatory case, the excursion occurred when the pressure pulses had subsided, as verified by the instrumentation downstream of the test section. When the oscillations disappeared at the outlet pressure transducer, they disappeared almost simultaneously at the two downstream thermocouples, the downstream transducer, and the downstream flowmeter, and annular flow or incomplete condensing appeared at the glass section near the entrance of the cooler. Figure 12(a) shows the coolant inlet temperature at which the interface undergoes this excursion as a function of the flow rate ratio. The coolant inlet temperature  $T_\ell$  at which the excursion occurs increases as the mass flow rate ratio  $m_r$  increases. The data fall on a line nearly parallel to, but above, the curve for the inception of the low-frequency oscillations (fig. 8(a)). These data may also be plotted on a coolant efficiency basis (fig. 12(b)), where the excursions would take place at lower coolant utilization factors for higher flow rate ratios.

The experimental points of the onset of both oscillatory and excursive instability for a set of runs are plotted on the same graph in figure 13, to define the regions of instability. In this figure, the plots are the coolant inlet subcooling  $T_v - T_\ell$  as a function of

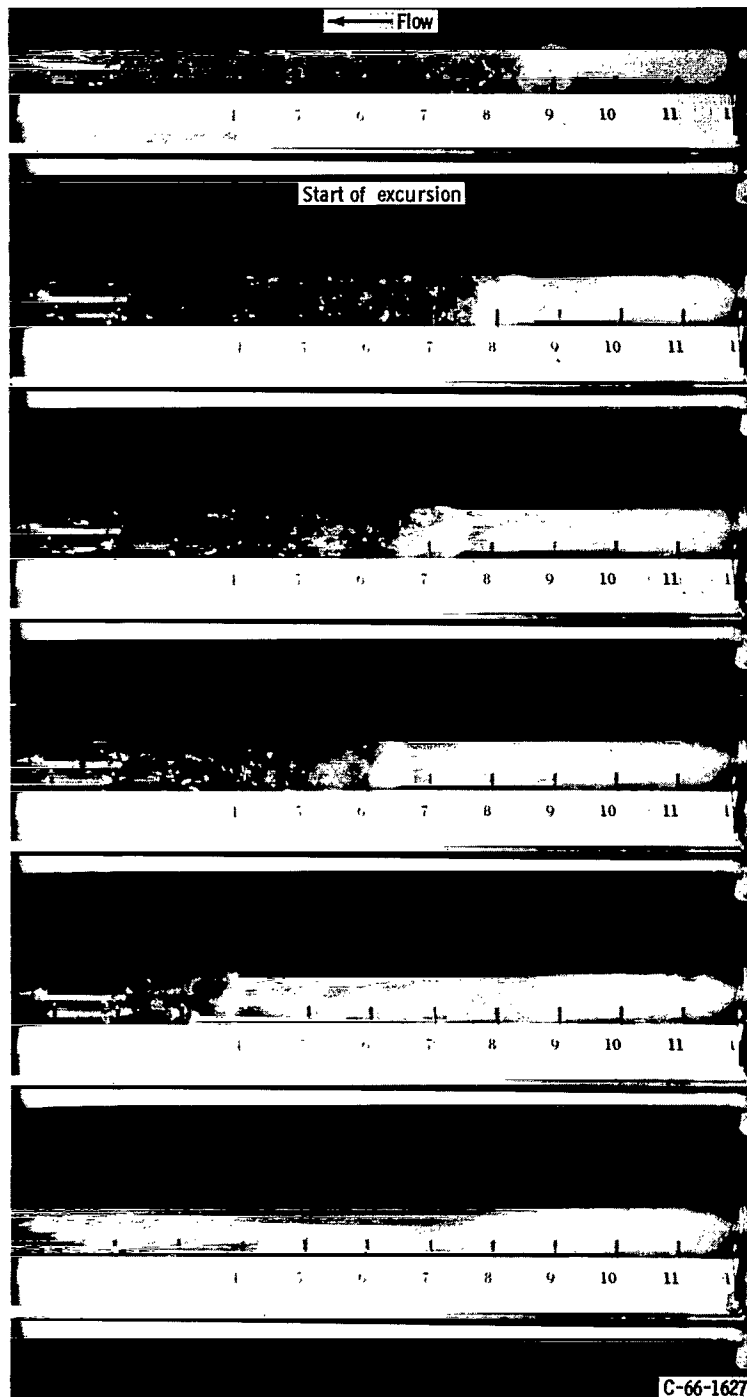


Figure 11. - Interface excursion phases in sequence.

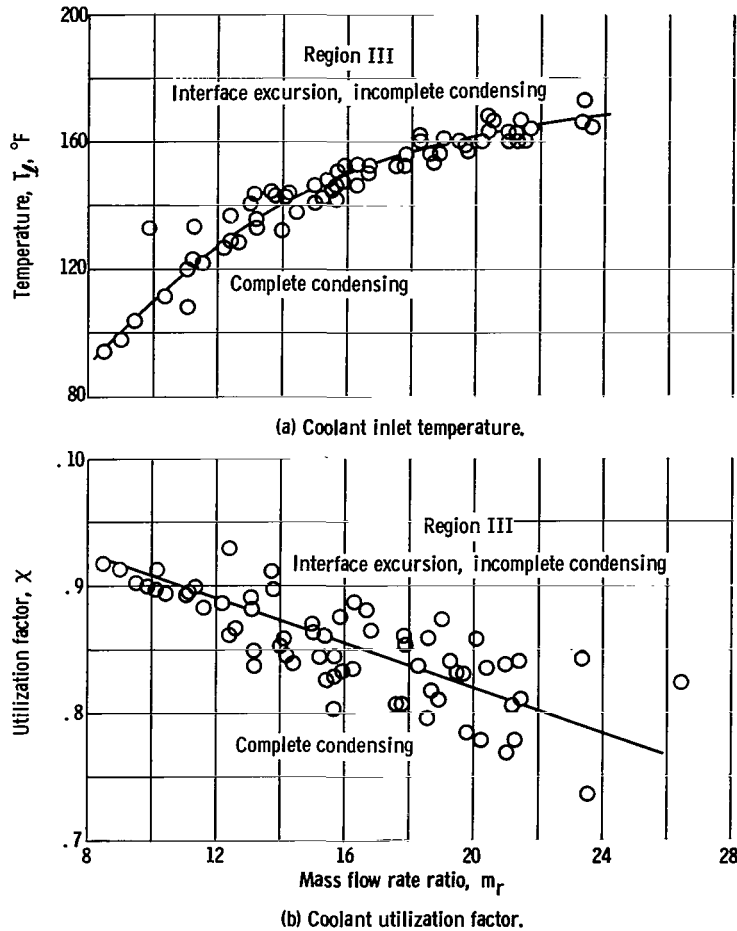


Figure 12. - Coolant temperature and utilization factor at which interface excursion occurs as function of mass flow rate ratio. Saturation pressure, approximately 17 pounds per square inch absolute.

the coolant flow rate  $\dot{M}_f$ , which is the form more commonly used for presenting boiling results. The general shape of the curves in figure 13 resembles that in the boiler stability plots of Gouse and Andrysiak (ref. 5), which show that the occurrence of boiling oscillations can be predicted by the independent variable, inlet subcooling.

### Comparison With Subcooled Boiling Instability

All three regions or modes of instability (random high-frequency pressure fluctuations, regular low-frequency oscillations, and interface excursions) have also been observed in subcooled boiling. In reference 3, the high-frequency fluctuations are also proposed to be caused by void collapse, and the effect of fluid temperature was the same as shown in figure 6 (p. 9). The amplitude of the fluctuations approaches zero as the inlet



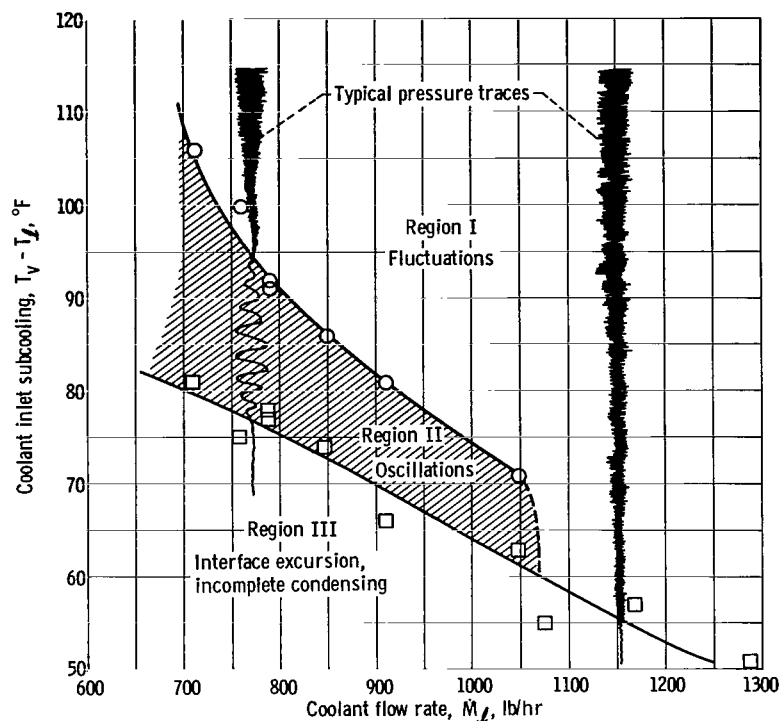


Figure 13. - Instability regions for typical set of runs. Saturation pressure, 17 pounds per square inch absolute  $\pm 3$  percent; vapor flow rate, 56 pounds per hour  $\pm 3$  percent.

coolant temperature increases (i. e., as the outlet temperature nears saturation).

Regular low-frequency oscillations of pressure and flow have also been observed in subcooled boiling (e. g., refs. 4 to 6). The low-frequency oscillations observed in subcooled boiling are similar to those that occur in region II of the pressure traces for this study. The similarities between this study and the boiling studies of reference 4 are seen in the shape of the pressure-time traces and the occurrence of a flow pattern transition from bubbly to annular flow at the inception of oscillations. The resemblance is seen also in the boiling stability regime curves, inlet subcooling as a function of flow rate (ref. 5). Interface excursions, which occurred at the end of the low-frequency oscillations, are present in boiling, but they are not considered to be an undesirable mode or instability because they denote nothing more than the development of a steady, annular flow pattern typical of certain net quality boiling and, hence, usually the desirable goal of the process. It was pointed out in reference 4 that the regular low-frequency oscillations associated with subcooled boiling could be suppressed by increasing the heat flux. This would result in net quality steam generation, which would seem to be analogous to the transition from oscillatory behavior to the interface excursion.

If subcooled boiling is considered to be contact condensing under a different configuration (in particular, in the experiments of ref. 4, where boiling was simulated by inject-

ing stream through a porous wall into the subcooled liquid), the observed similarities are not surprising.

## SUMMARY OF RESULTS

During the intermixing of steam with subcooled water in cocurrent streams, three distinct types of disturbances occurred, depending on the coolant temperature or coolant subcooling:

1. At low coolant inlet temperatures, there were irregular high-frequency pressure fluctuations, which are believed to have been caused by vapor void collapse. The amplitude of these disturbances decreased with increasing coolant temperature.

2. At a higher coolant temperature, regular, nearly sinusoidal low-frequency pressure, interface, and flow oscillations appeared. The coolant inlet temperature at which the oscillations began increased with coolant-flow-rate or flow-rate-ratio increases. The amplitude of the pressure oscillations varied in two ways:

- (a) For a constant pressure drop in the coolant line, the amplitude decreased as the coolant flow rate or flow rate ratio increased, and these oscillations disappeared completely at some high flow rate ratio.

- (b) For a constant coolant flow rate, the amplitude decreased with increasing pressure drop in the coolant line to a point after which increasing pressure drop had little effect, even at the maximum pressure drop of 90 pounds per square inch. At low pressure drops (up to 25 psi), the coolant flow also oscillated.

3. At a still higher coolant temperature, complete condensing in a relatively short distance was no longer possible, and the condensing interface underwent an excursion out of the test section. The coolant inlet temperature at which the excursion occurred increased with coolant flow rate increases.

4. Both the high- and low-frequency disturbances of this investigation were found to be similar to those encountered in subcooled boiling studies. The influential parameters appear to be the same for both boiling and condensing and similar stability maps are obtained.

Lewis Research Center,  
National Aeronautics and Space Administration,  
Cleveland, Ohio, April 14, 1966.

## APPENDIX A

### SYMBOLS

<b>A</b>	peak-to-peak amplitude of pressure oscillations, psi	<b><math>\chi</math></b>	coolant utilization factor, $(T_o - T_\ell)/(T_v - T_\ell)$ , nondimensional
<b><math>L_c</math></b>	condensing length, in.	<b>Subscripts:</b>	
<b><math>\dot{M}</math></b>	mass flow rate, lb/hr	<b>bi</b>	boiler inlet
<b><math>m_r</math></b>	ratio of coolant to vapor mass flow rate, $\dot{M}_\ell/\dot{M}_v$	<b>bo</b>	boiler outlet
<b>P</b>	pressure, psia	<b><math>\ell</math></b>	liquid coolant at inlet of test section
<b><math>\Delta P</math></b>	pressure drop, psi	<b>o</b>	test section outlet
<b>T</b>	temperature, $^{\circ}\text{F}$	<b>v</b>	vapor at inlet of test section

## APPENDIX B

### STABILITY OF MULTITUBE FORCED-FLOW BOILER

During the shakedown or initial operation period of the facility, the boiler was unstable. Since this instability could certainly affect the stability of the condenser, a stable operating region for the boiler had to be found. This minor boiler investigation yielded some interesting data that are presented in this appendix.

The boiler was a commercially built stainless-steel shell-and-tube heat exchanger consisting of 296 tubes (54 in. long, i. d. , 0. 214 in.) with 86. 5 square feet of heat transfer area, which was heated by pressurized hot water counter-circulated through the shell. The loop used for this study is shown schematically in figure 14.

When the boiler was unstable, the frequency of the pressure oscillations at the outlet was low (periods between 3 and 8 sec), and the peak-to-peak amplitude was as high as 3. 5 pounds per square inch. The actual trace shown in figure 15 is typical of all the oscillations and is characterized by a faster rise time than fall time and irregular high-frequency fluctuations, which appear on the pressure rise only. The high-frequency dis-

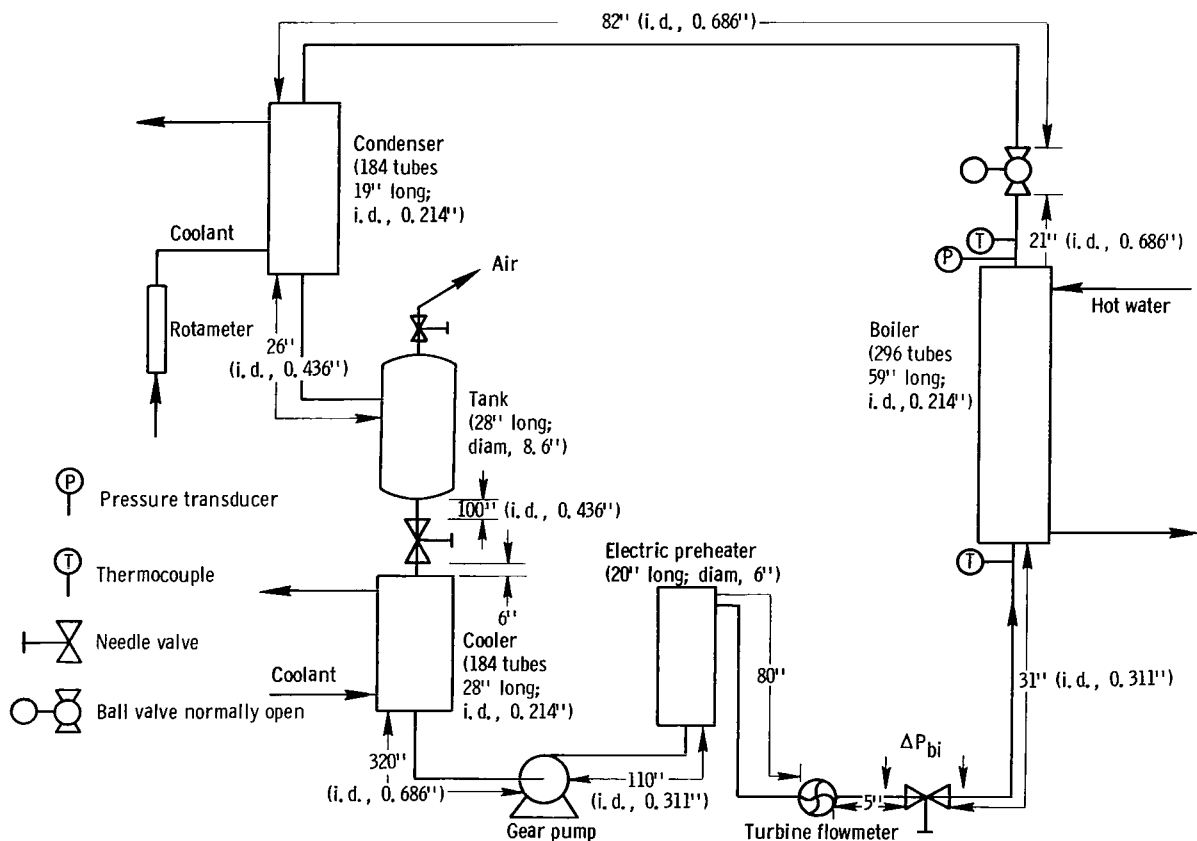


Figure 14. - Schematic illustration of multitube forced-flow boiler loop.

turbances during the pressure rise may be due to vapor bubble collapse caused by the suppression of the boiling that results from the increasing saturation pressure.

The effect of boiler outlet quality was investigated first. Since there was no preheating (i. e., boiler tube inlet temperature of approximately 65° F), little or no boiler tube inlet pressure drop  $\Delta P_{bi}$  and a relatively constant heat flux (within 10 percent), the liquid flow rate into the boiler could be varied to control the outlet quality. Figure 16 is a plot of the peak-to-peak value of the boiler outlet pressure fluctuations as a function of quality. The amplitude grew from 0.5 pound per square inch at 10 percent quality to about 3.5 pounds per square inch near 50 percent quality; it began to decrease as the quality proceeded above 50 percent. Although there are few data, especially in the high-quality region, it is believed that the amplitude does go to zero near 100 percent quality. This belief is based on the fact that the boiler was very stable in subsequent contact condenser runs (fig. 17), when the quality was 90 percent or better.

Since the maximum fluctuations occurred at qualities between 30 percent and 60 percent, qualities in this range were used in the investigation of the effect of boiler inlet pressure drop  $\Delta P_{bi}$ . Without preheating, there was little effect, as shown in the lower curve of figure 18. The peak-to-peak value of the outlet pressure oscillations  $A_{bo}$  went

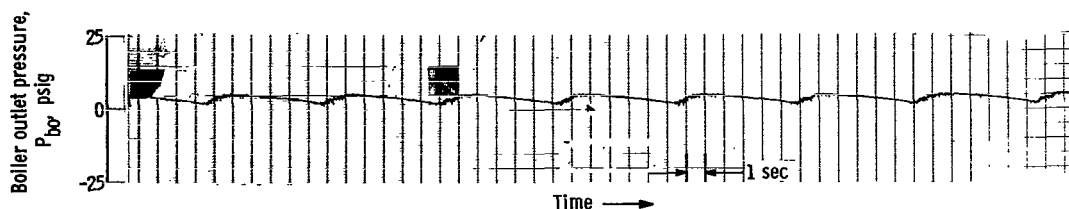


Figure 15. - Typical boiler outlet pressure oscillations.

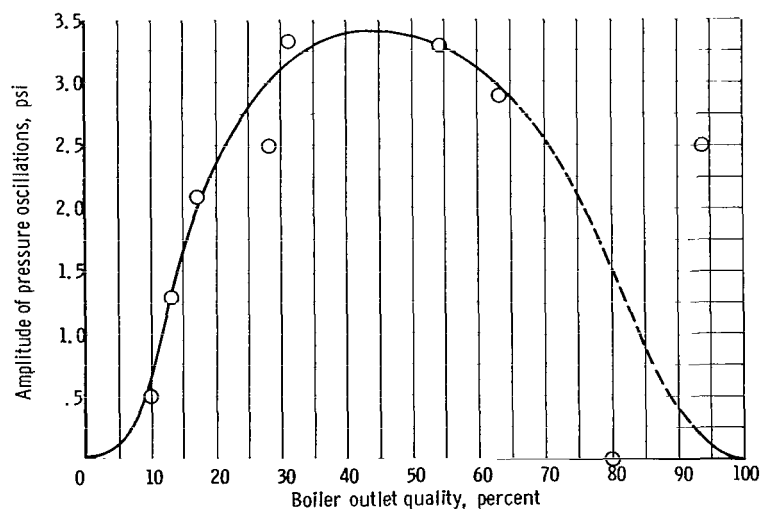


Figure 16. - Amplitude of boiler outlet pressure (peak-to-peak) oscillations as function of boiler exit quality.

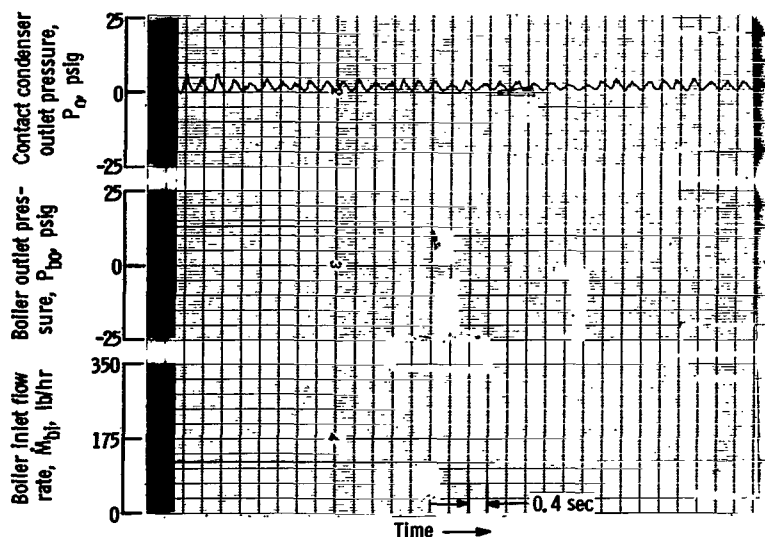


Figure 17. - Stable behavior of boiler operating during oscillatory instability in contact condenser.

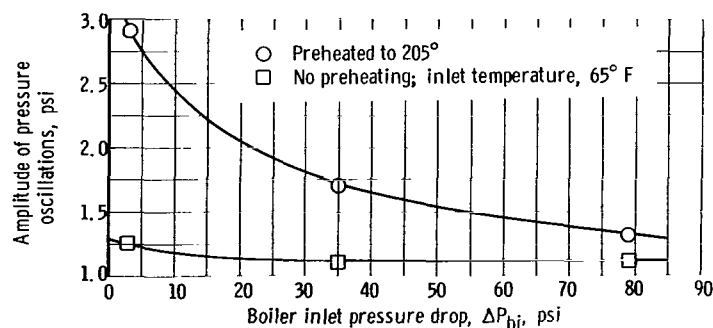


Figure 18. - Amplitude of boiler outlet pressure (peak-to-peak) oscillations as function of boiler inlet pressure drop with and without preheating.

from 1.25 to 1.10 pounds per square inch as  $\Delta P_{bi}$  was increased from 3 to 79 pounds per square inch. With preheating (boiler inlet temperature of about 205° F), there was a considerable  $\Delta P_{bi}$  effect. As  $\Delta P_{bi}$  was increased from 3 to 79 pounds per square inch,  $A_{bo}$  decreased from 2.9 to 1.3 pounds per square inch. Although increasing  $\Delta P_{bi}$  lowered the amplitude of the oscillations, it was still higher with preheating than without preheating for the same  $\Delta P_{bi}$ . Examples of data traces are shown in figures 19 and 20. At low  $\Delta P_{bi}$  (fig. 19), the flow oscillates in the preheater. Figure 20 shows the subsiding of oscillations as the inlet pressure drop is increased to 60 pounds per square inch. The other conditions for these figures are about the same (i. e., preheating to 205° F; exit quality, 90 percent).

While the preceding investigations were being conducted, it was observed that the coolant flow rate to the condenser was affecting the stability. If the boiler was stable

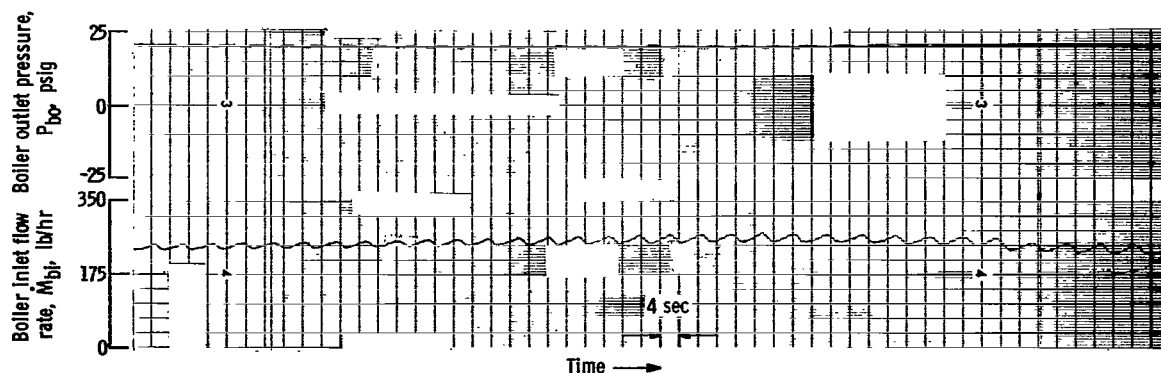


Figure 19. - Oscillatory instability in boiler. Preheating to 205° F; exit quality, 90 percent boiler inlet pressure drop, 2 pounds per square inch.

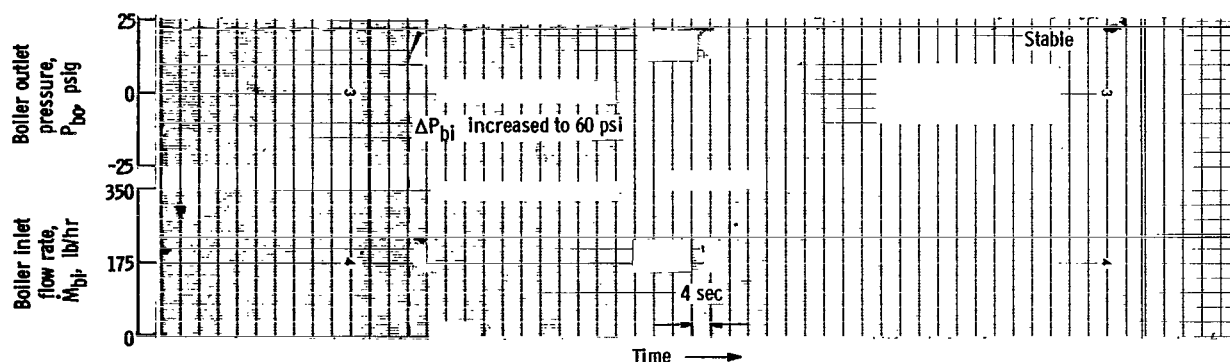


Figure 20. - Effect on boiler stability of increasing boiler inlet pressure drop to 60 pounds per square inch. Preheating to 205° F; exit quality, 90 percent.

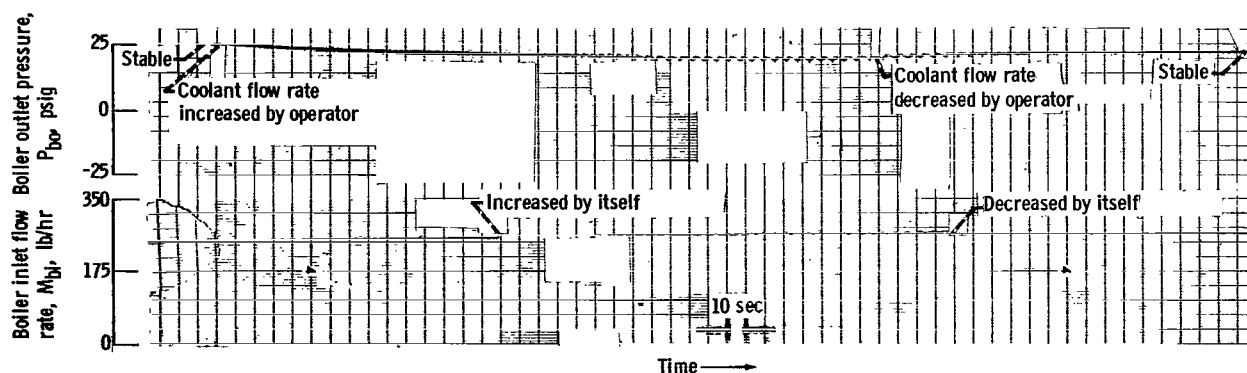


Figure 21. - Effect on boiler stability of condenser coolant flow rate.

(quality near 100 percent) and the coolant flow rate was increased, the boiler became unstable and could be stabilized by decreasing the coolant flow rate (fig. 21). One possible explanation of this is that as the condenser coolant flow rate increases the condenser pressure decreases and, hence, the boiler outlet pressure decreases, as shown in figure 21. This causes the latent heat of vaporization and the flow rate (experimentally verified in fig. 21) to increase, which in turn causes a decrease in quality; as was shown in figure 18, decreasing the quality from 100 percent causes instability.

As a result of this secondary investigation, it was found that stable boiler operating regions could be obtained by

- (1) Obtaining high qualities (90 percent or better)
- (2) Preheating to within  $40^{\circ}$  F of saturation (necessary for high qualities)
- (3) Maintaining large boiler inlet pressure drop (80 psi necessary for stability with preheating)



## REFERENCES

1. Hays, Lance: Investigation of Condensers Applicable to Space Power Systems. Pt. II. Jet Condensers. Rept. No. 1588, Electro-Optical Systems, Inc. (NASA CR-52862), 1962.
2. Platt, Robert J., Jr.: Investigation of a Jet Condenser for Space Power. NASA TN D-3045, 1965.
3. Jeglic, Frank A.; Stone, James R.; and Gray, Vernon H.: Experimental Study of Subcooled Nucleate Boiling of Water Flowing in 1/4-Inch-Diameter Tubes at Low Pressures. NASA TN D-2626, 1965.
4. Jeglic, Frank A.; and Grace, Thomas M.: Onset of Flow Oscillations in Forced-Flow Subcooled Boiling. NASA TN D-2821, 1965.
5. Gouse, S. William, Jr.; and Andrysiak, Carl D.: Flow Oscillations in a Closed Loop with Transparent, Parallel, Vertical, Heated Channels. Rept. No. 8973-2, M. I. T., June 24, 1963.
6. Daleas, R. S.; and Bergles, A. E.: Effects of Upstream Compressibility on Subcooled Critical Heat Flux. Paper No. 65-HT-67, ASME, 1965.
7. Goodykoontz, Jack H.; and Dorsch, Robert G.: Local Heat Transfer Coefficients for Condensation of Steam in Vertical Downflow Within a 5/8-Inch Tube. NASA TN D-3326, 1966.
8. Wyde, Sidney S.; and Kunz, H. R.: Experimental Investigation of Heat Rejection Problems in Nuclear Space Powerplants. Vol. II. Condensing Flow Stability Studies. Rept. No. PWA-2227, Pratt & Whitney Aircraft (NASA CR-55035), 1963.

*"The aeronautical and space activities of the United States shall be conducted so as to contribute . . . to the expansion of human knowledge of phenomena in the atmosphere and space. The Administration shall provide for the widest practicable and appropriate dissemination of information concerning its activities and the results thereof."*

—NATIONAL AERONAUTICS AND SPACE ACT OF 1958

## NASA SCIENTIFIC AND TECHNICAL PUBLICATIONS

**TECHNICAL REPORTS:** Scientific and technical information considered important, complete, and a lasting contribution to existing knowledge.

**TECHNICAL NOTES:** Information less broad in scope but nevertheless of importance as a contribution to existing knowledge.

**TECHNICAL MEMORANDUMS:** Information receiving limited distribution because of preliminary data, security classification, or other reasons.

**CONTRACTOR REPORTS:** Technical information generated in connection with a NASA contract or grant and released under NASA auspices.

**TECHNICAL TRANSLATIONS:** Information published in a foreign language considered to merit NASA distribution in English.

**TECHNICAL REPRINTS:** Information derived from NASA activities and initially published in the form of journal articles.

**SPECIAL PUBLICATIONS:** Information derived from or of value to NASA activities but not necessarily reporting the results of individual NASA-programmed scientific efforts. Publications include conference proceedings, monographs, data compilations, handbooks, sourcebooks, and special bibliographies.

*Details on the availability of these publications may be obtained from:*

SCIENTIFIC AND TECHNICAL INFORMATION DIVISION  
NATIONAL AERONAUTICS AND SPACE ADMINISTRATION  
Washington, D.C. 20546